Title

Integrative omics analysis suggests a prognostic role and potential mechanisms of miro1 in multiple myeloma

Authors names and affiliations:

Jiali Chu[1], Jing Zhu[1], Yan Yan[3], Haochen Liu[1], Liming Zheng[3], Ziyan Wang[1], Yunxi Liu[1], Ziyuan Gao[1], Li Lei[3], *Tianxiao Zhang[1,2], *Jinsong Hu[3]

[1] Department of Epidemiology and Biostatistics, School of Public Health, Xi'an Jiaotong University, Xi'an, 710061, China.

[2]Department of Geriatric Endocrinology Metabolism, Xi'an Jiaotong University Second Affiliated Hospital, Xi'an, 710004,China.

[3]Department of Genetics and Cell Biology,School of Basic Medical Sciences, Xi'an Jiaotong University, Xi'an, 710061, China.

****Correspondence Authors***

Tianxiao Zhang[1,2]

[1]Department of Epidemiology and Biostatistics, School of Public Health, Xi'an Jiaotong University, Xi'an, 710061, China.

[2]Department of Geriatric Endocrinology Metabolism, Xi'an Jiaotong University Second Affiliated Hospital, Xi'an, 710004,China.

E-mail: joshuaz@mail.xjtu.edu.cn

Jinsong Hu[3]

[3]School of Basic Medical Sciences, Xi'an Jiaotong University, Xi'an, 710061, China.

E-mail: jinsong.hu@xjtu.edu.cn

Abstract

Multiple myeloma (MM) is a hematological malignancy for which a definitive cure remains elusive. Despite initial responses to treatment, most patients eventually develop drug resistance and experience relapse, which significantly compromises their prognosis. Miro1 (RHOT1), a small GTPase localised in the outer mitochondrial membrane, plays an important role in regulating mitochondrial dynamics. However, its specific function in tumour lipid metabolism has not been clarified. We investigated the role of Miro1 in MM by integrating transcriptomic and lipidomic profiling in Miro1-overexpressing MM cells (Karpas-707). RNA-seq and Liquid Chromatography–Tandem Mass Spectrometry (LC-MS/MS) were used to identify differentially expressed genes and lipid species, and population-level analyses including survival and Mendelian randomization (MR) were performed based on data from public available databases. Functional enrichment and statistical analyses were carried out using established bioinformatics pipelines. Overexpression of Miro1 induces significant transcriptional changes, with 114 differentially expressed genes enriched in pathways including lipid metabolism. Lipidomics analysis identified 33 altered lipid species, notably within the phosphatidylcholine (PC) category, though these differences lost statistical significance after FDR correction. Kaplan-Meier survival analysis demonstrated that elevated RHOT1 expression correlates with poor prognosis in multiple myeloma patients. Molecular covariate analysis further revealed a significant positive causal association between RHOT1 expression and four phospholipid species, indicating a mechanistic link between Miro1 and phospholipid metabolism in multiple myeloma. This integrated study reveals a novel role for Miro1 in the pathological pathways of multiple myeloma, potentially through regulation of phospholipid metabolism. By modulating lipid metabolic pathways, Miro1 may serve concurrently as both a prognostic biomarker and a potential therapeutic target in multiple myeloma.

Keywords

Multiple myeloma; Miro1; Lipidomics; Transcriptomics; Mendelian Randomizatio

List of abbreviations

multiple myeloma (MM)

cis-acting expression quantitative trait loci (eQTL)

genome-wide association (GWAS)

Mendelian randomization (MR)

Inverse Variance Weighted (IVW)

Phosphatidylcholine(PC)

Introduction

Multiple myeloma (MM) is a haematological malignancy originating from bone marrow plasma cells, which is characterised by clonal proliferation of abnormal plasma cells and abnormal secretion of monoclonal immunoglobulins [1]. In recent years, with the continuous advancement of therapeutic methods, new therapies including immunomodulators, proteasome inhibitors, monoclonal antibodies, and chimeric antigen receptor T-cell immunotherapy (CAR-T) have been widely used in clinical practice[2], which have significantly prolonged the survival of MM patients [3]. However, MM is still regarded as an incurable disease with a high degree of genetic and phenotypic heterogeneity, and patients often experience drug resistance and relapse after initial remission [4]. This makes in-depth understanding of its pathogenesis and exploration of new molecular targets a key direction of current MM research.

Increasing evidence suggests that reprogramming of lipid metabolism profoundly shapes cancer progression[5] and therapeutic response by altering the tumor microenvironment (TME)[6].In MM, tumor cells stimulate lipolysis in adipocytes, releasing free fatty acids (FFAs) that are efficiently taken up through specific fatty acid transporters[7]. These FFAs not only serve as energy sources but also help MM cells adapt to immune and nutrient stress, thereby promoting tumor growth and survival[8].However, the molecular mechanisms underlying lipid metabolic reprogramming in MM remain incompletely understood.

Miro1 (encoded by RHOT1, a mitochondrial Rho GTPase 1) is a small GTPase localized in the outer mitochondrial membrane [9]. Its unique structural features, such as the EF-hand calcium-binding structural domain, allow it to regulate mitochondrial function in multiple ways[10].By sensing changes in intracellular calcium concentration, these structural domains regulate mitochondrial localization and movement, thereby affecting their distribution and transport across the cytoskeleton[11].Recent studies have shown that enhancing Miro1-driven mitochondrial transport, or inducing mitochondrial depolarization by accelerating its

degradation process, can help to alleviate oxidative stress and inflammatory responses, and thus alleviate a variety of neurological disorders[12].In addition, it has been shown that Miro1, by regulating mitochondrial localization, enables localized energy supply, thereby supporting dynamic changes in cell membranes, cytoskeletal remodeling, and the formation and stabilization of adhesion patches, which play a key role in high-energy-demanding processes such as cell migration [13].Recent studies also suggest that Miro1 may maintain mitochondrial functional integrity by inhibiting mitochondrial autophagy under lipotoxic stress conditions[14] and may be involved in the regulation of peroxisomes[15], suggesting that it may have an important regulatory role in lipid metabolism. However, the specific function of Miro1 in lipid metabolism and its association with the pathogenesis of multiple myeloma (MM) remain to be further investigated.

In this study, we aimed to explore the role of Miro1 in lipid metabolism and its clinical significance in MM. By integrating transcriptomic and lipidomic analyses of Miro1-overexpressing MM cells, together with survival analysis of MM patients and MR analysis of genetic data, we sought to elucidate the molecular mechanisms by which Miro1 modulates lipid metabolism, and to evaluate its potential as both a prognostic biomarker and a therapeutic target in MM.

Materials and Methods

In this study, we performed combined transcriptomic and lipidomic analyses on Kapas-707 cells with high Miro1 expression to identify the key pathways it affects. Subsequently, the potential causal relationship between Miro1 and lipid metabolism-related metrics was assessed by combining survival analysis and two-sample Mendelian randomization analysis based on Genome-Wide Association Study(GWAS) data. The study design was summarized in Figure 1.

The human MM cell line Karpas-707 (Cellosaurus accession: CVCL_0010), derived from patient bone marrow, was obtained from a certified cell bank[16] and cultured in RPMI-1640 medium supplemented with 10% fetal bovine serum (FBS) and 1% penicillin–streptomycin at 37℃ in a humidified incubator with 5% CO_2.To

investigate the biological effects of Miro1 overexpression, Karpas-707 cells were transduced with lentiviral constructs encoding Miro1 (*RHOT1*) (OE-Miro1 group) or an empty vector (EV group) as control. Each experimental condition included at least three biological replicates to ensure reproducibility and statistical power.

Transcriptomic Profiling and Bioinformatic Analysis

Total RNA was extracted using TRIzol and assessed for integrity before library preparation with the Illumina mRNA kit.Libraries were sequenced on the Illumina platform to obtain paired-end FASTQ reads. After quality control to remove adapters, low-quality bases, and contaminants, reads were aligned to the human reference genome (GRCh38.112) using HISAT2.Transcript assembly and quantification were performed with StringTie, and expression levels reported as FPKM and TPM [17].

Differential expression analysis was conducted with DESeq2,defining significant genes as adjusted *P*-value<0.05 and |log2FC| $\geqslant$ 1. Expression values were log-transformed and scaled before statistical analysis. Functional enrichment of DEGs was carried out using clusterProfiler for GO and KEGG analyses [18], with FDR<0.05 considered significant [19].Volcano plots and heatmaps were generated in R with ggplot2 and pheatmap.Detailed methods of transcriptomic analyses are provided in the Supplementary Methods.

Lipidomic Profiling and Bioinformatic Analysis

Cell samples were processed through methanol/MTBE-based extraction, followed by centrifugation and reconstitution for LC-MS/MS analysis. Liquid chromatography was conducted using a Ultra Performance Liquid Chromatography (UPLC) system coupled with a C30 column under a specific gradient elution protocol. Mass spectrometric detection employed a QTRAP® 6500+ LC-MS/MS system with Electrospray Ionization (ESI) in both positive and negative ion modes. Multiple Reaction Monitoring (MRM) was used to detect lipid species, with detailed tuning and calibration for optimized detection.

The analysis included unsupervised PCA performed using the R function prcomp on unit variance-scaled data [20].Differential metabolites were selected based on VIP > 1 and *P*-value <0.05 from Orthogonal Projections to Latent Structures-Discriminant

Analysis (OPLS-DA) results generated by MetaboAnalystR[21], with log transformation and mean centering applied.Metabolites were annotated using the KEGG Compound database and mapped to KEGG Pathway for enrichment analysis, with significance determined by hypergeometric test *P*-values[22].Lipidomics data analysis was performed using the R language package, which mainly uses the Z-score standardization and centering method to process the data and supports multivariate statistical analysis and visualization. Detailed methods of lipid metabolomic analyses are provided in the Supplementary Methods.

Survival and Mendelian Randomization Analysis

Kaplan–Meier survival analysis[23] was performed using RNA-seq transcript per million (TPM) data from the MMRF-CoMMpass cohort[24].The data sets obtained from University of California, Santa Cruz (UCSC) Xena (http://xenabroswer.net/hub).Patients with MM were stratified into high and low *RHOT1* expression groups based on TPM values. Overall survival (OS) differences between the two groups were evaluated using the log-rank test.

To assess the causal effect of Miro1 (*RHOT1*) expression on lipid metabolism, we obtained cis-acting eQTL data from the GTEx portal (https://gtexportal.org)[25] and aggregated lipid GWAS statistics from the GWAS catalogue and Integrative Epidemiology Unit (IEU)OpenGWAS platform (https://gwas.mrcieu.ac.uk)[26].SNPs associated with *RHOT1* expression ($P < 5 \times 10^{-6}$) were filtered for linkage disequilibrium ($r^2 < 0.001$) and instrument strength ($F > 10$). Bivariate MR analysis was performed using R software (TwoSampleMR, v4.4.2), employing inverse variance weighting (IVW) as the primary estimator [27], supplemented by MR-Egger regression [28], weighted median [29], and weighted mode [30]methods. Cochran's Q test assessed heterogeneity,whilst MR-Egger intercept[31] and MR-PRESSO[32] evaluated multiplicity effects. Forest plots and scatterplots visualised causal estimates. Multiple testing correction employed the Benjamini-Hochberg method, with FDR < 0.05 deemed significant [33].

Results

Differential Gene Expression in Miro1-Overexpressing MM Cells

Differential gene expression analysis revealed 114 DEGs in Miro1-overexpressing cells compared to the control group(Supplementary Table S1), including 27 upregulated and 87 downregulated genes (adjusted *P*-value<0.05, |log2FC|≥1) (Figure 2A). Hierarchical clustering of the top 60 DEGs showed clear separation between samples (Figure 2B). Notably, genes such as *MBOAT2, CAVIN2, FADS1, LRP1,* and *ITPR3* were significantly altered and are functionally enriched in lipid metabolism and calcium signaling pathways.

Based on differentially expressed genes (DEGs), we performed KEGG, GO, and GSEA functional enrichment analyses. KEGG analysis（Supplementary Figure S1） revealed significant enrichment in pathways such as ECM-receptor interaction, focal adhesion, and PI3K-Akt signaling, indicating potential involvement in disease-related processes. GO enrichment (Supplementary Figure S2) showed that DEGs were mainly enriched in the plasma membrane, extracellular exosome, and neuronal cell body, suggesting that high Miro1 expression may affect membrane remodeling and vesicle-mediated intercellular communication. GSEA analysis (Supplementary Figure S3) indicated enrichment trends in pathways like TGF-β signaling, inflammatory response, and oxidative phosphorylation, though these did not reach statistical significance after multiple testing correction and require further validation.

Miro1-Induced Changes in Lipid Composition Revealed by Lipidomic Data

Lipidomic profiling revealed 1,148 lipid metabolites in total, of which 33 exhibited significant changes in Miro1-overexpressing cells (25 downregulated and 8 upregulated) (Figure 3). PCA and OPLS-DA analyses further highlighted clear separation between the OE-Miro1 and EV groups, and the significant metabolites were characterized by VIP>1 and *P*-value < 0.05. Among the most upregulated species were Phosphatidylcholine (O-16:0_14:1) and Phosphatidylcholine (16:1_17:1), while Phosphatidylglycerol (18:1_21:1) and Phosphatidylserine (18:1_19:1) were the most downregulated. None of the metabolite changes remained significant after FDR

correction.KEGG enrichment analysis (Supplementary Figure S4) revealed enrichment trends in key pathways such as glycerophospholipid metabolism, neurotrophin signaling pathway, and adipocytokine signaling pathway, although none reached statistical significance after multiple testing correction.

High RHOT1 Expression Predicts Poor Prognosis in MM Patients

Patients with high *RHOT1* expression exhibited significantly shorter overall survival compared to those with low expression (*P*-value < 0.05) (Figure 4). These findings suggest that elevated *RHOT1* expression may serve as a negative prognostic biomarker in MM.

Causal Influence of RHOT1 on Phosphatidylcholine (PC) Metabolism: Evidence from MR

MR analysis indicated that *RHOT1* expression may causally influence PC species.This inference was based on 24 independent SNPs used as instrumental variables (Supplementary Table S2).The inverse-variance weighted (IVW) method revealed significant positive associations between *RHOT1* expression and several PC subtypes(Figure 5), including PC(14:0_18:2) (OR = 1.14, 95% CI: 1.05 – 1.24, *P*-value = 0.002, *P*-FDR = 0.040), PC(18:0_22:6) (OR = 1.15, *P*-value = 0.001, *P*-FDR= 0.039), PC(O-18:0_14:0) (OR = 1.17, *P*-value = 0.001, *P*-FDR = 0.028), and PC(O-18:0_16:1) (OR = 1.16, *P*-value = 0.002, *P*-FDR = 0.040). No significant associations were detected using alternative MR methods(Supplementary Table S3).Cochran's Q test and MR-Egger regression detected no significant heterogeneity or horizontal pleiotropy MR-PRESSO and sensitivity analyses further confirmed the robustness of the results (Supplementary Table S4).

Discussion

In this study, we investigated the role of Miro1 (*RHOT1*) in regulating lipid metabolism in MM using multi-omics data, survival analysis and MR analysis. The results showed that there were differentially expressed genes associated with lipid metabolism in the transcriptomic data of the Miro1 high-expression group, and that high Miro1 expression significantly shortened the overall survival of MM patients. In addition, there was a causal association between Miro1 and four PC lipids, suggesting

that Miro1 may influence the progression of MM through lipid metabolic pathways.

Mitochondria acquire phospholipids from the endoplasmic reticulum via endoplasmic reticulum-mitochondria contact sites (EMCSs). Miro1, a small GTPase located on the mitochondrial outer membrane, not only regulates mitochondrial transport along the cytoskeleton to facilitate its association with the endoplasmic reticulum, but also plays a crucial role in mitochondrial dynamics, energy maintenance, and calcium homeostasis. [9-12], though its specific role in tumour metabolism remains unclear. Transcriptomic analysis revealed that Miro1 overexpression induces significant transcriptional alterations in multiple myeloma cells, identifying 114 differentially expressed genes (DEGs). DEGs induced by Miro1 overexpression were enriched in networks including the PI3K-Akt signaling pathway and focal adhesions. The PTEN-PI3K/Akt pathway is recognised as a key molecular pathway in malignant cell progression and development [34]. Previous studies have demonstrated the role of integrin-β 7 in MM cell adhesion [35].These findings suggest that Miro1 may promote disease progression by regulating these signaling pathways and influencing MM cell adhesion, proliferation, and migration. GO enrichment analysis further indicates that DEGs are significantly enriched in the plasma membrane, exosomes, and neuronal cytoplasm, suggesting Miro1 may participate in membrane lipid biogenesis, vesicular transport, and metabolic signal transduction across cells [15]. Previous studies have demonstrated that in hematological malignancies, exosome release influences interactions between tumor cells and other cells, thereby promoting disease progression by suppressing immune responses and triggering drug resistance [36]. Consequently, Miro1 may regulate metabolic adaptation processes by influencing extracellular signal perception and transduction systems.

Statistical significance of differential lipid metabolites was no longer significant after FDR correction for lipid metabolome. Meta-analyses have shown that higher lipid levels (e.g. Low-Density Lipoprotein (LDL), High-Density Lipoprotein (HDL), total cholesterol, and triglycerides) are associated with a reduced risk of MM, and in particular, higher triglyceride levels are causally associated with MM risk[37]. Thus changes in key lipid molecules such as PC (16:1_17:1) and PG (18:1_21:1) suggest

that Miro1 may be involved in the regulation of membrane lipid dynamics by modulating glycerophospholipid and PC synthesis pathways.

As a major component of the cell membrane, phosphatidylcholine (PC) plays a pivotal role in rapidly proliferating tumour cells, not only participating in membrane synthesis but also regulating T cell activation, protein kinase C signalling pathways, and immune responses [38]. Research indicates that PC can suppress $CD8^+$ T cell infiltration and cytotoxic function via the lysophosphatidic acid pathway, thereby weakening antitumour immunity [39]. Furthermore, as a vital component of the mitochondrial membrane[40], PC not only maintains mitochondrial membrane structural integrity but also supports mitochondrial function by regulating inner membrane protein transport and energy metabolism[41][42]. Particularly within the nervous system, PC deficiency may lead to mitochondrial dysfunction, disrupting energy supply and metabolic homeostasis[43].Another MR study indicated that multiple myeloma correlates positively with serum triglyceride and phosphatidylinositol levels, whereas elevated phosphatidylethanolamine, phosphatidylcholine, and sterol ester levels are associated with reduced disease risk [44]. The MR analysis in this study similarly demonstrated a significant positive causal relationship between *RHOT1* expression levels and four PC molecules, which remained statistically significant after FDR correction. This suggests that Miro1 may constitute a novel pro-tumour mechanism by promoting PC synthesis, enhancing membrane synthesis capacity, exacerbating immune evasion, or improving metabolic adaptability. Concurrently, Kaplan-Meier analysis revealed significantly reduced overall survival in patients with high *RHOT1* expression, further underscoring its potential value as an adverse prognostic factor at the clinical outcome level. Combining transcriptomic and lipidomic findings at the cellular level, these discoveries collectively indicate that Miro1 may influence membrane lipid dynamics by regulating glycerophospholipid and PC synthesis pathways. Survival analysis and MR analysis at the population level further validate this hypothesis.

The present study suffered from certain limitations. The lipidomic analysis failed to reach statistical significance after FDR correction, which needs to be validated by

expanding the sample size in the future. In addition, despite the strong causal inference ability of MR analyses, the SNP data of the instrumental variables used were mainly from European populations, and the population limitation of the samples may have some impact on the results. Further studies are still needed to validate the specific metabolic pathways mediated by Miro1 and analyze its role in other aspects of the membrane.

Conclusions

The present study reveals a novel role for Miro1 in the pathological pathways of multiple myeloma by regulating lipid metabolism. Through modulating lipid metabolic pathways, Miro1 may function as both a prognostic biomarker and a potential therapeutic target in multiple myeloma. These findings indicate that Miro1 promotes MM progression by modulating phospholipid metabolism, highlighting its potential as a prognostic marker and therapeutic target.

Declarations

Ethics approval and consent to participate

All data used in this study were obtained from publicly available databases. No new human or animal subjects were involved, and ethical approval was not required.

Consent for publication

Consent for publication is not applicable for this article.

Availability of data and materials

The original data presented in this study are openly available. The eQTL data from whole blood and small intestine tissues were obtained from the eQTLGen Consortium(https://www.eqtlgen.org/)[25].Summary-level GWAS data were extracted from the GWAS Catalog(https://www.ebi.ac.uk/gwas/)[26], including a dataset comprising 377,277 samples (Study IDs: GCST90277238 – GCST90277416).

Competing interests

The authors declare no competing interests. The funding sources had no role in the study design, data collection and analysis, manuscript preparation, or publication decision.

Funding

This study was supported by the Shanxi Province Science and Technology Research and Development Program (2024SF-YBXM-14).

Authors' contributions

JLC and TXZ conceived and designed the study. JLC and JZ analyzed and interpreted data. YY and HCL performed the experiments following the established methodology and conducted the experiments. LMZ and ZYW were responsible for data visualization. Supervision was provided by YXL, ZYG, and LL. The original draft was written by JLC and the manuscript was reviewed and edited by TXZ and JSH. All authors confirm the authenticity of all the raw data. All authors read and approved the final version of the manuscript.

Acknowledgments

We acknowledge the support of Shaanxi Province Science and Technology Research and Development Program.

References

[1] Cowan AJ, Green DJ, Kwok M, et al. Diagnosis and Management of Multiple Myeloma: A Review. JAMA. 2022;327(5):464-477.
[2] Rodriguez-Otero P, Ailawadhi S, Arnulf B, et al. Ide-cel or Standard Regimens in Relapsed and Refractory Multiple Myeloma. N Engl J Med. 2023;388(11):1002-1014.
[3] Lu Q, Yang D, Li H, Niu T, Tong A. Multiple myeloma: signaling pathways and

targeted therapy. Mol Biomed. 2024;5(1):25.
[4] Swamydas M, Murphy EV, Ignatz-Hoover JJ, Malek E, Driscoll JJ. Deciphering mechanisms of immune escape to inform immunotherapeutic strategies in multiple myeloma. J Hematol Oncol. 2022;15(1):17.
[5] Corn KC, Windham MA, Rafat M. Lipids in the tumor microenvironment: From cancer progression to treatment. Prog Lipid Res. 2020;80:101055.
[6] Yang K, Wang X, Song C, et al. The role of lipid metabolic reprogramming in tumor microenvironment. Theranostics. 2023;13(6):1774-1808.
[7] Panaroni C, Fulzele K, Mori T, et al. Multiple myeloma cells induce lipolysis in adipocytes and uptake fatty acids through fatty acid transporter proteins. Blood. 2022;139(6):876-888.
[8] Torcasio R, Gallo Cantafio ME, Ikeda RK, Ganino L, Viglietto G, Amodio N. Lipid metabolic vulnerabilities of multiple myeloma. Clin Exp Med. 2023;23(7):3373-3390.
[9] Boulton DP, Caino MC. Emerging roles for Mitochondrial Rho GTPases in tumor biology. J Biol Chem. 2024;300(9):107670.
[10] Panchal K, Tiwari AK. Miro (Mitochondrial Rho GTPase), a key player of mitochondrial axonal transport and mitochondrial dynamics in neurodegenerative diseases. Mitochondrion. 2021;56:118-135.
[11] Baltrusaitis EE, Ravitch EE, Fenton AR, Perez TA, Holzbaur ELF, Dominguez R. Interaction between the mitochondrial adaptor MIRO and the motor adaptor TRAK. J Biol Chem. 2023;299(12):105441.
[12] Schuler MH, Lewandowska A, Caprio GD, et al. Miro1-mediated mitochondrial positioning shapes intracellular energy gradients required for cell migration. Mol Biol Cell. 2017;28(16):2159-2169.
[13] Zeng L, Yang J, Zhang C, et al. Miro1: A potential target for treating neurological disorders. Neuroscience. 2025;577:228-239.
[14] Alshaabi H, Shannon N, Gravelle R, Milczarek S, Messier T, Cunniff B. Miro1-mediated mitochondrial positioning supports subcellular redox status. Redox Biol. 2021;38:101818.
[15] Li JM, Li X, Chan LWC, et al. Lipotoxicity-polarised macrophage-derived exosomes regulate mitochondrial fitness through Miro1-mediated mitophagy inhibition and contribute to type 2 diabetes development in mice. Diabetologia. 2023;66(12):2368-2386.
[16] Karpas A, Fischer P, Swirsky D. Human myeloma cell line carrying a Philadelphia chromosome. Science. 1982;216(4549):997-999.
[17] Hao D, Wang X, Wang X, Thomsen B, Kadarmideen HN, Lan X, Huang Y, Chen H. Transcriptomic changes in bovine skeletal muscle cells after resveratrol treatment. Gene. 2020 Sep 5;754:144849.
[18] Yu G, Wang LG, Han Y, He QY. clusterProfiler: an R package for comparing biological themes among gene clusters. OMICS. 2012 May;16(5):284-7.
[19] Szklarczyk D, Gable AL, Nastou KC, Lyon D, Kirsch R, Pyysalo S, Doncheva NT, Legeay M, Fang T, Bork P, Jensen LJ, von Mering C. The STRING database in 2021: customizable protein-protein networks, and functional characterization of

user-uploaded gene/measurement sets. Nucleic Acids Res. 2021 Jan 8;49(D1):D605-D612.
[20] Palumbo L, Fiorito S, Epifano F, Sharifi-Rad M, Genovese S, Collevecchio C. Solid-phase adsorption methodologies of naturally occurring anthraquinones: A review. Phytochem Anal. 2023 Mar;34(2):153-162.
[21] Lyu X, Wang Y, Xu Y, Zhao Z, Liu H, Hu Z. Metabolomic Profiling of Tumor Tissues Unveils Metabolic Shifts in Non-Small Cell Lung Cancer Patients with Concurrent Diabetes Mellitus. J Proteome Res. 2024 Sep 6;23(9):3746-3753.
[22] Huckvale E, Moseley HNB. kegg_pull: a software package for the RESTful access and pulling from the Kyoto Encyclopedia of Gene and Genomes. BMC Bioinformatics. 2023 Mar 4;24(1):78.
[23] Beis G, Iliopoulos A, Papasotiriou I. An Overview of Introductory and Advanced Survival Analysis Methods in Clinical Applications: Where Have we Come so far? Anticancer Res. 2024 Feb;44(2):471-487.
[24] Skerget S, Penaherrera D, Chari A, et al. Comprehensive molecular profiling of multiple myeloma identifies refined copy number and expression subtypes. Nat Genet. 2024;56(9):1878-1889.
[25] Barbeira AN, Bonazzola R, Gamazon ER, et al. Exploiting the GTEx resources to decipher the mechanisms at GWAS loci. Genome Biol. 2021;22(1):49.
[26]Bai Y, Wang X, Xu Y, et al. Vitamin D and Gestational Diabetes Mellitus in the IEU OpenGWAS Project: A Two-Sample Bidirectional Mendelian Randomization Study. Nutrients. 2024;16(17):2836.
[27] Mounier N, Kutalik Z. Bias correction for inverse variance weighting Mendelian randomization. Genet Epidemiol. 2023;47(4):314-331.
[28] Ding M, Zhang Z, Chen Z, Song J, Wang B, Jin F. Association between periodontitis and breast cancer: two-sample Mendelian randomization study. Clin Oral Investig. 2023;27(6):2843-2849.
[29] Ni F, Liu X, Wang S. Impact of negative emotions and insomnia on sepsis: A mediation Mendelian randomization study. Comput Biol Med. 2024;180:108858.
[30] Sang N, Gao RC, Zhang MY, Wu ZZ, Wu ZG, Wu GC. Causal Relationship Between Sleep Traits and Risk of Systemic Lupus Erythematosus: A Two-Sample Mendelian Randomization Study. Front Immunol. 2022;13:918749.
[31] Liu Z, Wang H, Yang Z, Lu Y, Zou C. Causal associations between type 1 diabetes mellitus and cardiovascular diseases: a Mendelian randomization study. Cardiovasc Diabetol. 2023;22(1):236.
[32] Li J, Cheng C, Zhang J. Autoimmune diseases and the risk of bladder cancer: A Mendelian randomization analysis. J Autoimmun. 2024;146:103231.
[33] Liang J, Liu G, Wang W, Xue H. Causal relationships between gut microbiota and lymphoma: a bidirectional Mendelian randomization study. Front Cell Infect Microbiol. 2024;14:1374775.
[34] Zhang Y, Zheng L, Ding Y, et al. MiR-20a Induces Cell Radioresistance by Activating the PTEN/PI3K/Akt Signaling Pathway in Hepatocellular Carcinoma. Int J Radiat Oncol Biol Phys. 2015;92(5):1132-1140.
[35] Neri P, Ren L, Azab AK, et al. Integrin β7-mediated regulation of multiple

myeloma cell adhesion, migration, and invasion. Blood. 2011;117(23):6202-6213.
[36] Allegra A, Di Gioacchino M, Tonacci A, Petrarca C, Musolino C, Gangemi S. Multiple Myeloma Cell-Derived Exosomes: Implications on Tumorigenesis, Diagnosis, Prognosis and Therapeutic Strategies. Cells. 2021;10(11):2865.
[37] Zhu W, Charwudzi A, Li Q, Zhai Z, Hu L, Pu L. Lipid levels and multiple myeloma risk: insights from Meta-analysis and mendelian randomization. Lipids Health Dis. 2024;23(1):299.
[38] Saito RF, Andrade LNS, Bustos SO, Chammas R. Phosphatidylcholine-Derived Lipid Mediators: The Crosstalk Between Cancer Cells and Immune Cells. Front Immunol. 2022;13:768606.
[39] Yan W, Shi X, Zhao Y, Liu X, Jia X, Gao L, Yuan J, Liao A, Yasui H, Wang X, Wang X, Zhang R, Wang H. Microbiota-reprogrammed phosphatidylcholine inactivates cytotoxic CD8 T cells through UFMylation via exosomal SerpinB9 in multiple myeloma. Nat Commun. 2025 Mar 24;16(1):2863.
[40]Modi HR, Katyare SS. Effect of treatment with cadmium on structure-function relationships in rat liver mitochondria: studies on oxidative energy metabolism and lipid/phospholipids profiles. J Membr Biol. 2009;232(1-3):47-57.
[41]Schuler MH, Di Bartolomeo F, Mårtensson CU, Daum G, Becker T. Phosphatidylcholine Affects Inner Membrane Protein Translocases of Mitochondria. J Biol Chem. 2016;291(36):18718-18729.
[42] Li XQ, Han Yumei, Zhou S, Cheng JF. Advances in Understanding Therapeutic Mechanisms of Exercise Interventions for Individuals with Comorbid Depression and Cardiovascular Diseases: A Narrative Review. Heart and Mind. 2024;8(4):292-299. DOI:10.4103/hm.HM-D-24-00036.
[43]von Maydell D, Wright SE, Pao PC, et al. ABCA7 variants impact phosphatidylcholine and mitochondria in neurons. Nature. Published online September 10, 2025.
[44] Zhong Y, Li Y, Sun W, Xiao M. Liposomes have a direct effect on multiple myeloma: a Mendelian randomization study. Front Oncol. 2024 Jun 11;14:1404744.

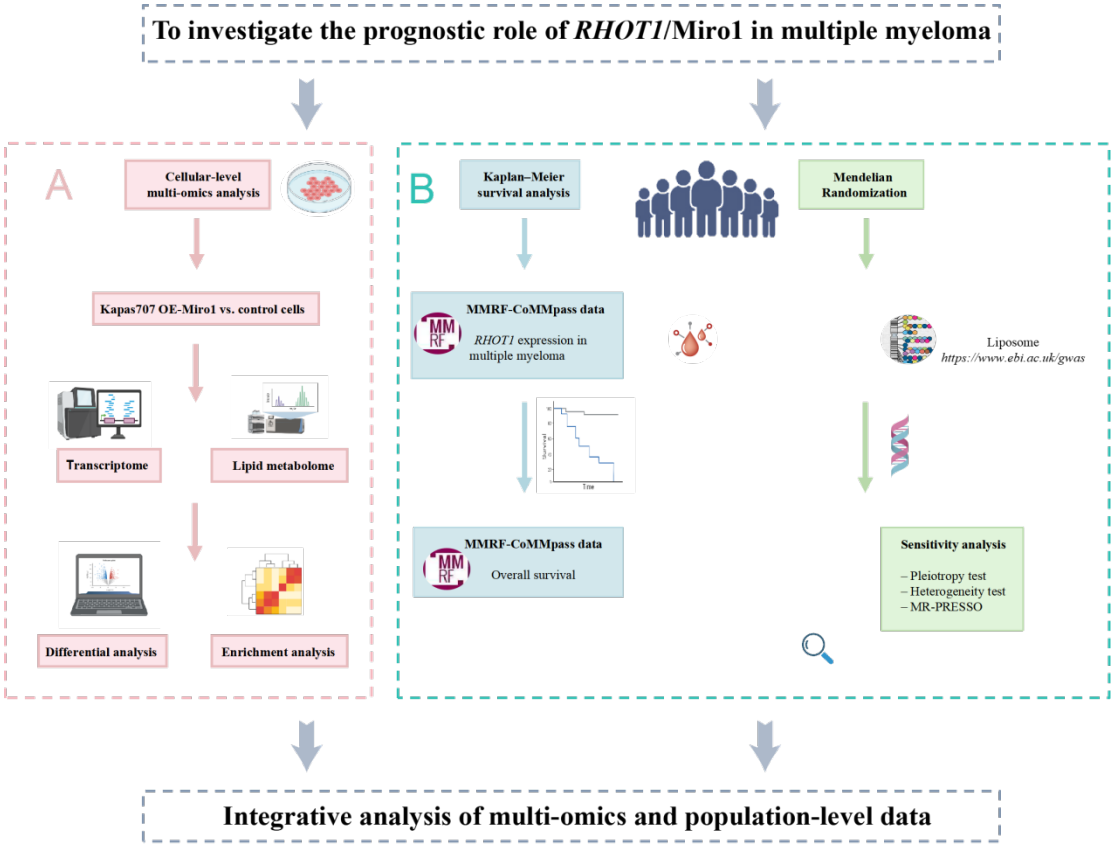

Figure 1.Overview of the Study Design

(A)Cellular-level multi-omics analysis: Transcriptomic and lipidomic profiling were performed on Kapas707 cells overexpressing Miro1 (OE-Miro1) and vector control cells to identify differentially expressed genes and metabolites. Enrichment analysis was conducted to explore the affected pathways.

(B) Population-level data analysis: Survival analysis using Kaplan–Meier curves was performed based on RHOT1 expression levels in the MMRF-CoMMpass dataset. A two-sample Mendelian randomization (MR) analysis was conducted to investigate the potential causal relationship between RHOT1 expression (exposure) and lipid metabolism-related traits (outcome) based on GWAS summary data.The main MR method was inverse-variance weighted (IVW), with MR-Egger, weighted median, weighted mode, and simple mode used as supplementary methods. Sensitivity analyses included pleiotropy and heterogeneity tests, as well as MR-PRESSO to detect potential outliers.

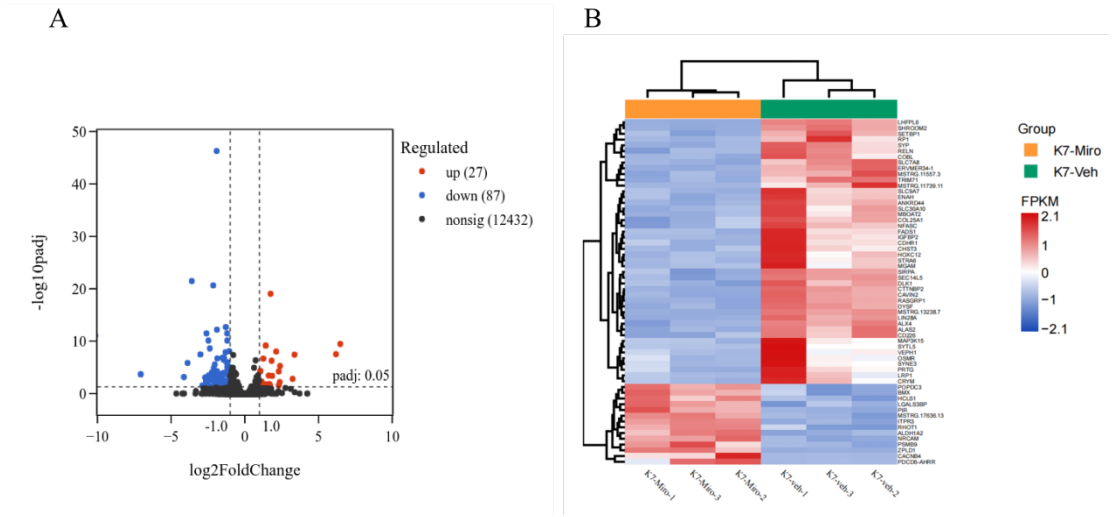

Figure 2. Differential gene expression and clustering analysis induced by Miro1 overexpression

(A)Volcano plot of differentially expressed genes (DEGs)

(B) Heatmap of top 60 DEGs ranked by adjusted P-value

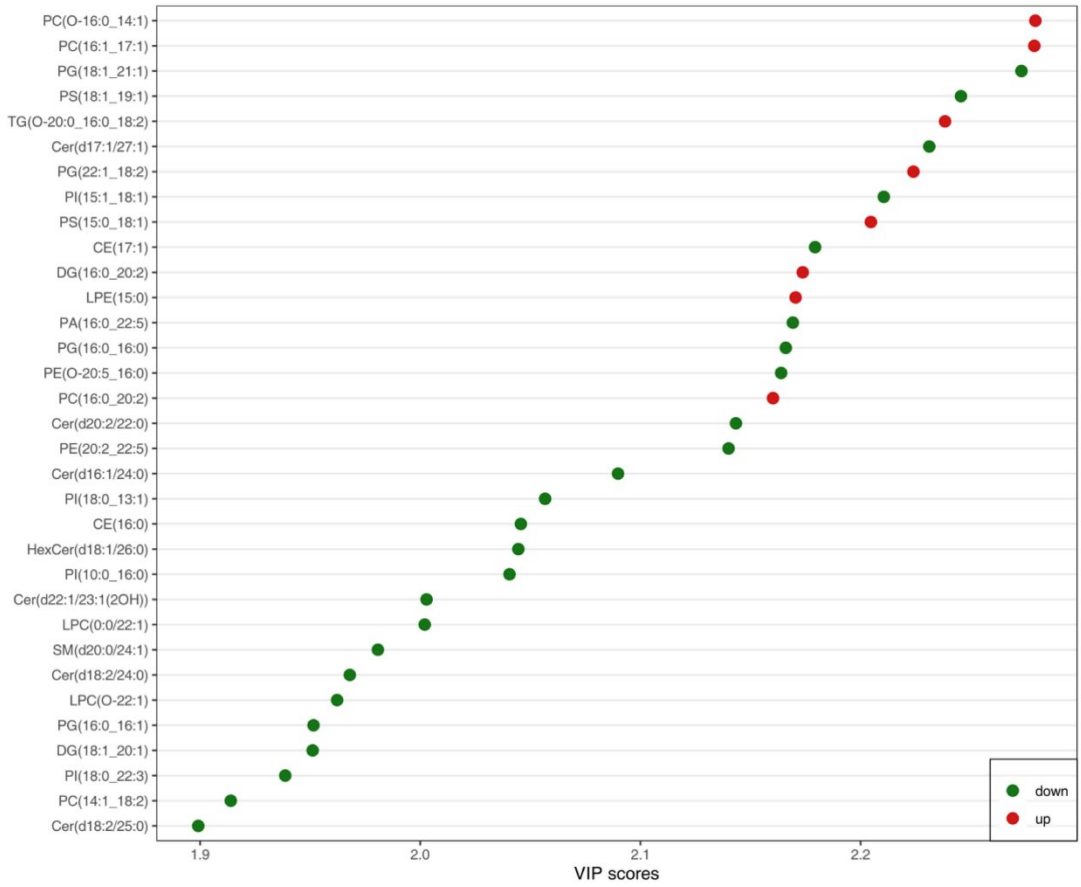

Figure 3. Differential lipid metabolite profiling based on VIP scores from OPLS-DA analysis

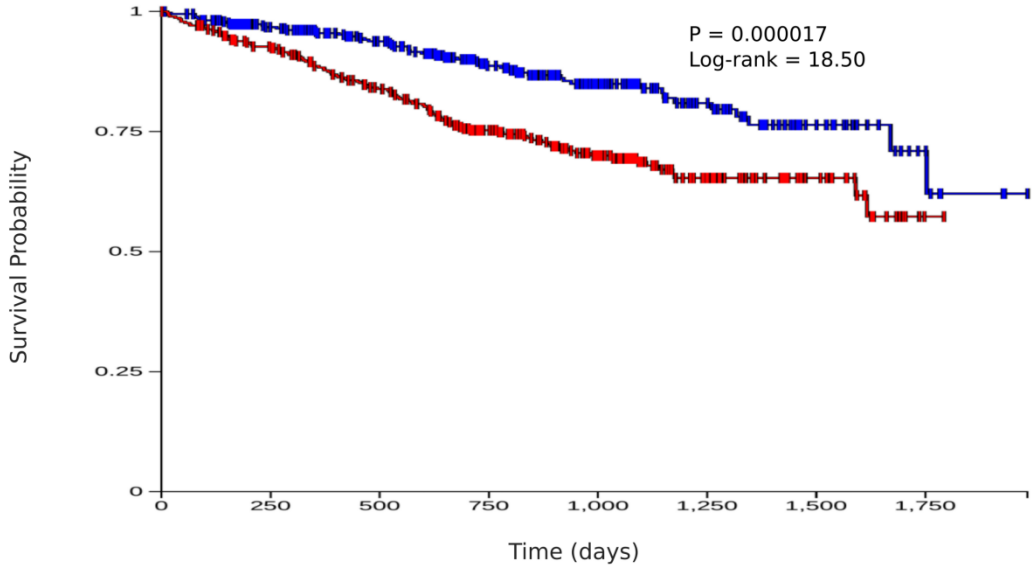

Time (days)	0	250	500	750	1000	1250	1500	1750
< 2.830	382	319	266	194	121	65	25	9
≥ 2.830	382	327	275	200	128	65	27	9

Figure 4. Kaplan-Meier Survival by RHOT1 Expression in Multiple Myeloma (RNA-seq, TPM)

Outcome	SNP(n)	Methods	Forest Plot	OR(95%CI)	Beta	P-value	P-FDR
Phosphatidylcholine (14:0_18:2)	24	MR Egger	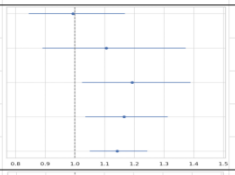	0.99 (0.84-1.17)	-0.0065	0.938	0.988
	24	Simple mode		1.11 (0.89-1.37)	0.1006	0.371	0.882
	24	Weighted mode		1.19 (1.02-1.39)	0.1763	0.033	0.926
	24	Weighted median		1.17 (1.03-1.31)	0.1531	0.011	0.293
	24	Inverse variance weighted		1.14 (1.05-1.24)	0.1333	0.002	0.040
Phosphatidylcholine (18:0_22:6)	24	MR Egger	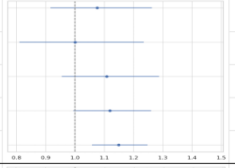	1.08 (0.92-1.26)	0.0729	0.383	0.988
	24	Simple mode		1.00 (0.81-1.24)	0.0004	0.997	0.997
	24	Weighted mode		1.11 (0.95-1.29)	0.1031	0.189	0.926
	24	Weighted median		1.12 (0.99-1.26)	0.1127	0.062	0.502
	24	Inverse variance weighted		1.15 (1.06-1.25)	0.1389	0.001	0.039
Phosphatidylcholine (O-18:0_14:0)	24	MR Egger	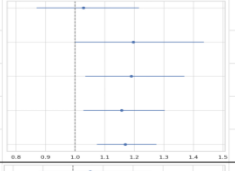	1.03 (0.87-1.22)	0.0279	0.746	0.988
	24	Simple mode		1.20 (1.00-1.44)	0.1794	0.066	0.882
	24	Weighted mode		1.19 (1.03-1.37)	0.1739	0.023	0.926
	24	Weighted median		1.16 (1.03-1.30)	0.1462	0.015	0.293
	24	Inverse variance weighted		1.17 (1.07-1.27)	0.1568	0.000	0.028
Phosphatidylcholine (O-18:0_16:1)	24	MR Egger	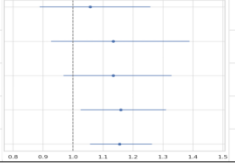	1.06 (0.89-1.26)	0.0559	0.535	0.988
	24	Simple mode		1.13 (0.93-1.39)	0.1260	0.234	0.882
	24	Weighted mode		1.13 (0.97-1.33)	0.1260	0.132	0.926
	24	Weighted median		1.16 (1.03-1.31)	0.1478	0.018	0.293
	24	Inverse variance weighted		1.16 (1.06-1.26)	0.1442	0.002	0.040

Figure 5. Forest plots of Mendelian Randomization analysis of RHOT1 Gene on Phosphatidylcholine Subtypes

Abbreviations: OR, odds ratio; CI, confidence interval; P-FDR,adjusted P-value